Journal of
Materials Chemistry A

RSC Publishing

PAPER

View Article Online
View Journal | View Issue

Published on 18 October 2013. Downloaded by Harvard University on 21/02/2014 20:11:26.

Cite this: J. Mater. Chem. A, 2013, **1**, 15416

Nitrogen-doped cuprous oxide as a p-type hole-transporting layer in thin-film solar cells†

Yun Seog Lee,[a] Jaeyeong Heo,[bc] Mark T. Winkler,[a] Sin Cheng Siah,[a] Sang Bok Kim,[b] Roy G. Gordon[b] and Tonio Buonassisi*[a]

Received 3rd September 2013
Accepted 17th October 2013

DOI: 10.1039/c3ta13208k

www.rsc.org/MaterialsA

We demonstrate the potential of a nitrogen-doped cuprous oxide (Cu_2O:N) film as a p-type hole-transporting layer for photovoltaic devices. To reduce back-contact resistance and create an electron-reflecting back surface field, high carrier density and appropriate work function are desired for the layer. Its electrical and optical properties can be appropriately tuned *via* nitrogen-doping to create a semi-transparent tunnel junction to a back-contact. We fabricate Cu_2O-based heterojunction thin-film solar cells and insert a 20 nm-thick Cu_2O:N hole-transporting layer between a silver back-contact and a Cu_2O light-absorbing layer. The insertion of a 20 nm-thick Cu_2O:N layer results in sizeable enhancements of fill-factor and power conversion efficiency of the solar cells. Cu_2O:N thin-films may also be useful in other photovoltaic material systems, improving their back-contact properties as well as widening the range of possible back-contact materials.

Introduction

Thin-film solar cells comprise a promising renewable-energy source due to their low material usage (compatible with tera-watts-level deployment) and potential for inexpensive manufacturing.[1,2] To develop high-efficiency photovoltaic devices, appropriate band alignment throughout the entire device structure is necessary to minimize energy losses from non-ideal interfaces. Most materials for light-absorbing layers are p-type, possess low carrier density, and often have deep valence band edge positions, which can result in unfavourable band alignment and a highly resistive Schottky barrier formation between the absorber layer and metal or transparent conducting oxide electrode.[3,4] To mitigate the absorber/electrode interface problems, hole-transporting layers have been introduced at the back-contact of various device types.[5–9] The layers are required to have high carrier density and appropriate band position to reduce contact resistance and create an "electron-reflecting" back surface field to promote carrier collection. Various transition-metal oxides including molybdenum oxide (MoO_3) and vanadium oxide (V_2O_5) have shown promising properties as hole-transporting layers due to their high work functions (Φ).[7–9] However, hole-selective and electron-blocking functions are limited due to their n-type nature and deep-lying states.[10]

p-Type doping of metal oxides is generally challenging, due to self-compensation and dopant solubility limits.[11,12] However, theoretical calculations predict that a few intrinsically p-type oxides can be extrinsically doped to be p^+-type.[13] Cuprous oxide (Cu_2O) is one such intrinsically p-type semiconductor with conduction band edge (E_C) and valence band edge (E_V) positions at 3.2 and 5.2 eV from the vacuum level, respectively.[14] With the addition of extrinsic acceptors, the Fermi level (E_F) can be further shifted toward E_V, without lowering the formation energies of compensating defects to negative values.[13] Various dopants including nitrogen, silicon, germanium, and some transition metals have been tested to increase the p-type conductivity of Cu_2O thin-films.[15–18] Among those elements, nitrogen is expected to substitute oxygen with a high solubility, given their similar ionic radii. Previously reported nitrogen doping has been shown to reduce electrical resistivity of Cu_2O by a factor of $\sim$100.[18] Thus, we hypothesize that it is possible to tune the electrical and optical properties of a nitrogen-doped Cu_2O (Cu_2O:N) layer and to incorporate it into a thin-film photovoltaic device as a hole-transporting layer to reduce back-contact resistance. In principle, such a layer could widen the range of possible back-contact materials suitable for solar-cell device fabrication, by reducing the severity of the so-called "roll-over" (current saturation at high forward bias).[19]

In this work, we demonstrate the potential of a nanometer-scale Cu_2O:N film as a p-type hole-transporting layer for photovoltaic devices. By controlling the nitrogen content in the film, carrier density and optical transmittance are tuned to form a low contact-resistance interface with minimal optical

[a]Massachusetts Institute of Technology, Cambridge, MA 02139, USA. E-mail: buonassisi@mit.edu
[b]Department of Chemistry and Chemical Biology, Harvard University, Cambridge, MA 02138, USA
[c]Department of Materials Science and Engineering, Chonnam National University, Gwangju 500-757, Korea

† Electronic supplementary information (ESI) available. See DOI: 10.1039/c3ta13208k

 This journal is © The Royal Society of Chemistry 2013

Published on 18 October 2013. Downloaded by Harvard University on 21/02/2014 20:11:26.

absorption. We fabricate Cu_2O-based metal–oxide heterojunction thin-film solar cells and insert a 20 nm-thick Cu_2O:N hole-transporting layer between a silver back-contact and a Cu_2O absorber layer. We select silver as a back-contact electrode, because its high reflectance around a wavelength of 550 nm enhances light trapping near the bandgap of Cu_2O and the peak of the solar spectrum. Despite the relatively low work function of silver and resulting resistive contact to intrinsic Cu_2O, the Cu_2O:N layer forms a tunnel junction that reduces the contact resistance due to its high carrier concentration. We demonstrate the addition of a Cu_2O:N layer results in sizeable enhancements of fill-factor (FF) and power conversion efficiency (PCE) relative to a control device without the layer.

Results and discussion

Nitrogen-doped Cu_2O thin-film growth

To incorporate nitrogen into Cu_2O thin-films, we used reactive magnetron sputtering. Reactive sputtering of metallic copper using O_2 and N_2 as reactive gases has been widely used for Cu_2O and copper nitride (Cu_3N) thin-film depositions.[20,21] We investigated a range of substrate temperatures during film growth ranging from 130 to 390 °C; 230 °C provided the lowest electrical resistivity of Cu_2O:N films (Fig. S1†). Substrate temperatures higher than 230 °C resulted in higher resistivities due to lower hole-densities. To control the nitrogen content, the N_2 flow rate was varied from 0 to 6 sccm, while the Ar and O_2 flow rates were fixed to 40 and 11 sccm for high-purity Cu_2O deposition. Fig. 1a shows the nitrogen content in the 0.6 μm-thick Cu_2O films measured by secondary ion mass spectrometry (SIMS). A controlled amount of nitrogen was implanted into an undoped Cu_2O thin-film sample and a Si wafer for calibrating the measured data. As the N_2 flow rate increased to 6 sccm, the nitrogen concentration ([N]) increased in an approximately linear fashion to 1.7 at.% (1.3×10^{21} cm^{-3}). If all the nitrogen doping were substitutional at oxygen sites, this doping level would correspond to replacing about 5% of the oxygen atoms by nitrogen atoms.

Structural and chemical properties of the host material (Cu_2O) were maintained for all nitrogen doses in our study. X-ray diffraction (XRD) measurement shows (111) and (200) peaks from the cubic structure of Cu_2O for the 0.6 μm-thick undoped and doped ([N] = 1.7 at.%) films (Fig. 1b). The Cu_2O:N film exhibited reduced peak intensities as [N] increased in the film, indicating lower crystallinity than the Cu_2O film. Peaks from metallic copper, cupric oxide (CuO), and Cu_3N were not detected in the measurement. X-ray photoelectron spectroscopy (XPS) was used to investigate chemical states of elements in the films. Cu $2p_{3/2}$ and $2p_{1/2}$ peaks at 932.8 ± 0.2 and 952.7 ± 0.2 eV shown in Fig. 1c indicate the same Cu oxidation state (Cu^{1+}) for

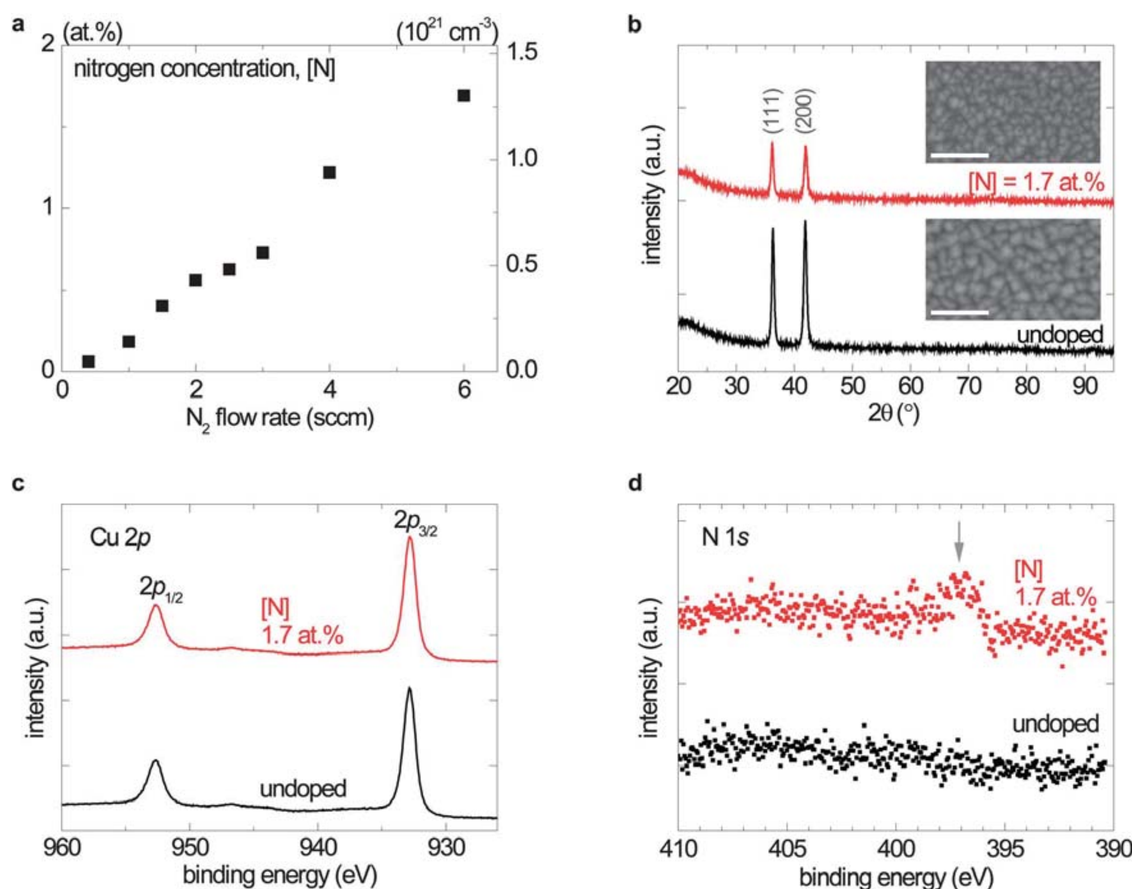

Fig. 1 (a) Nitrogen concentrations in Cu_2O:N films measured by SIMS. A typical calibration error range is up to ±30%. (b) XRD spectra of Cu_2O and Cu_2O:N films, indicating two main peaks from Cu_2O (111) and (200). Inset: SEM images of the sputtered Cu_2O (bottom) and Cu_2O:N (top) films. Both scale bars represent 300 nm. XPS spectra of (c) copper and (d) nitrogen core levels of Cu_2O and Cu_2O:N films. The arrow indicates a small nitrogen peak at 397.1 ± 0.2 eV.

Published on 18 October 2013. Downloaded by Harvard University on 21/02/2014 20:11:26.

Cu_2O and Cu_2O:N films. CuO peaks from Cu^{2+} states in the range 940–945 eV were not detected.[22] Due to the low sensitivity of XPS measurement to light elements, the signal from nitrogen was difficult to resolve. A small peak position from the nitrogen core level in the Cu_2O:N film ([N] = 1.7 at.%) was observed at 397.1 ± 0.2 eV (Fig. 1d), close to the nitrogen signal from Cu_3N (397.4 eV).[23] The peak position suggests that a considerable fraction of nitrogen in the Cu_2O:N film bonds with Cu^{1+}, as a substitution for oxygen.

Electrical and optical characteristics

The effects of nitrogen-doping on electrical and optical properties are shown in Fig. 2. In Fig. 2a, the measured electrical resistivity exhibits a strong reduction as more nitrogen is doped into the Cu_2O films. While the undoped Cu_2O film exhibits a resistivity of 1.4×10^2 Ω cm, the highest nitrogen dose (1.7 at.%) reduces the resistivity to 1.8×10^{-1} Ω cm, which is the lowest value among reported Cu_2O:N thin films to the knowledge of the authors. We carried out temperature-dependent Hall measurements to further elucidate the carrier properties of these films. All films with [N] up to 1.2 at.% show p-type conductivities; the film with [N] = 1.7 at.% could not be measured as the Hall voltage was too small due to its low mobility and high carrier concentration. Cu_2O:N films exhibited reduced mobility as [N] increased in the films (Fig. S2†), due to an increased density of ionized scattering centers.[20] Fig. 2b shows hole densities (p) increase to 1.1×10^{19} cm^{-3} at 300 K as the nitrogen content increases to 0.62 at.%. The hole densities show strong dependence on temperature. We estimate the carrier activation energies (E_A) by fitting the data to a compensated semiconductor model with a low-temperature approximation:

$$p = (2\pi m^* kT/h^2)^{3/2}[(N_A/N_D) - 1]\exp(-E_A/kT) \quad (1)$$

where m^* is the effective mass, k is Boltzmann's constant, h is Planck's constant, N_A is the acceptor density, and N_D is the donor density.[20,24] Cu_2O:N films with [N] greater than 0.06 at.% exhibited a decreased E_A of 0.12 eV (Fig. S3†). On the other hand, undoped Cu_2O and lightly doped Cu_2O:N ([N] = 0.06 at.%) films exhibited E_A of 0.18–0.19 eV, indicating that the dominating acceptor state moves close to the valence band at higher [N].[17,20]

As a result of the increased carrier density, carrier transport between Cu_2O:N and the Ag electrode can be enhanced. Metals normally exhibit unfavourable Schottky barriers at metal/Cu_2O interfaces except high work function metals (*e.g.* Au and Pt).[25,26]

The dominating carrier transport mechanism can be categorized by the parameter E_{00}, which can be defined as:

$$E_{00} = \frac{q\hbar}{2}\sqrt{\frac{p}{m^*\varepsilon}} \quad (2)$$

for p-type semiconductor, where q is the electron charge, $\hbar$ is the reduced Planck's constant, and ε is the dielectric constant of Cu_2O.[27,28] When the hole density in the Cu_2O film exceeds 10^{19} cm^{-3} ($E_{00} \gg kT$), the barrier width in Cu_2O is reduced sufficiently to form a tunnel junction, thereby field-emission dominates the carrier transport.[27,28] Temperature-dependent specific contact resistances (ρ_c) between Ag and Cu_2O:N films were measured using the circular transmission line model (CTLM) as shown in Fig. S4.†[29] The film exhibited a reduced ρ_c of 2.9×10^{-4} Ω cm^2 at room temperature as [N] increased to 1.2 at.%, while an undoped Cu_2O film exhibited a ρ_c of 1.9×10^{-2} Ω cm^2. The temperature dependence of ρ_c became weaker for the film with [N] = 1.2 at.%, indicating that field-emission

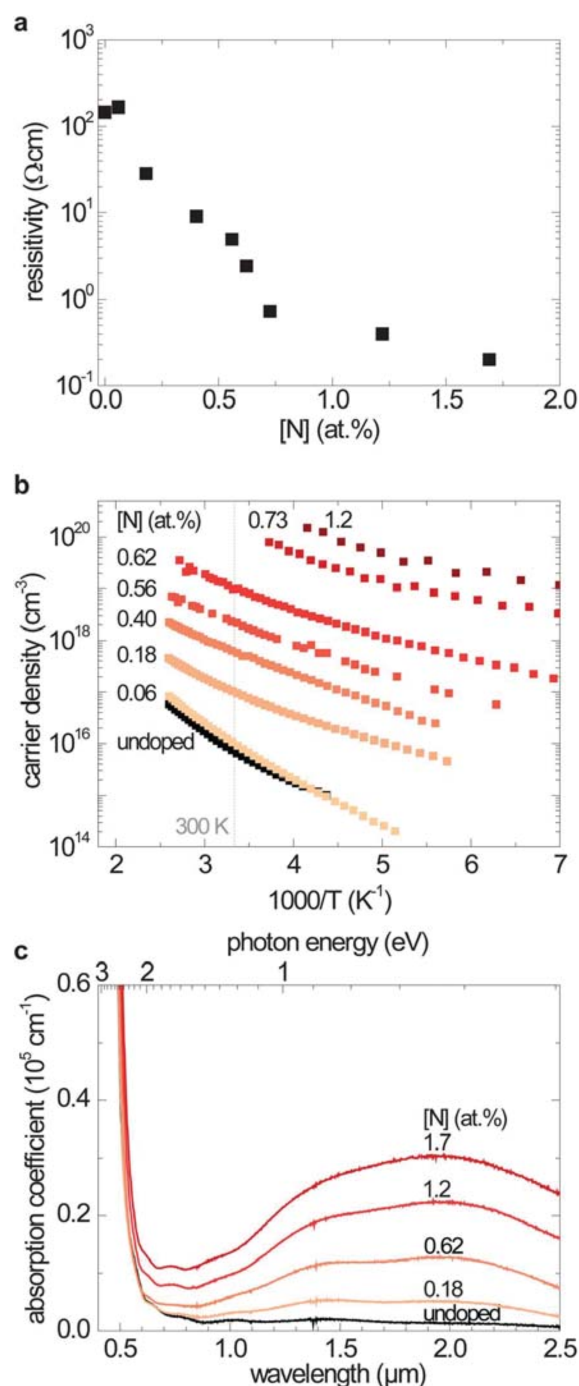

Fig. 2 Effects of nitrogen-doping on electrical and optical properties of Cu_2O:N films. (a) Electrical resistivity measured by a four-point-probe. (b) Temperature-dependence of carrier (hole) density determined by Hall-effect measurements. (c) Optical absorption coefficient of Cu_2O:N films measured by a spectrophotometer with an integrating sphere and a single-pass configuration.

This journal is © The Royal Society of Chemistry 2013

rather than thermionic-emission is dominating the carrier transport at the interface.[4]

To utilize Cu_2O:N as a hole-transporting layer, optical absorption by the layer needs to be minimized by tuning its absorption properties and layer thickness. We examined the effect of nitrogen doping on the optical absorption of Cu_2O:N films. As shown in Fig. 2c, the Cu_2O:N film exhibits a higher optical absorption coefficient (α) than the undoped Cu_2O film. In particular, a significant increase of α in the subgap wavelength region ($\lambda > 0.6$ μm) was observed for Cu_2O:N films. Zhao *et al.* suggested that substitutional nitrogen doping could increase the absorption near 1.7 eV ($\lambda = 0.73$ μm) by first-principles calculations.[30] However, the Cu_2O:N films in this study exhibited a broad absorption peak near ~0.6 eV ($\lambda \approx 2$ μm), and the peak intensity increased with the nitrogen content in the films. Similar absorption characteristics were reported for Cu_2O:N thin-films and were attributed to the nitrogen-induced subgap states.[18] Structural defects from the lower crystallinity of the Cu_2O:N films could also increase α over this wavelength range. Due to the increases in α, a 20 nm-thick Cu_2O:N ([N] = 1.2 at.%) layer would yield a hole-transporting layer with a total optical absorption lower than 5% of the AM1.5G solar spectrum for a wavelength range of 0.3–1.5 μm.

Thin-film solar cells with a Cu_2O:N hole-transporting layer

Using a 20 nm-thick Cu_2O:N layer ([N] = 1.2 at.%) as an interlayer between the Ag electrode and a Cu_2O absorber layer, we fabricated metal–oxide thin-film solar cells. Fig. 3a shows a cross-sectional scanning electron microscopy (SEM) image of the heterojunction solar cell. Cu_2O, amorphous zinc-tin-oxide (a-ZTO), and Al-doped ZnO (ZnO:Al) layers were used as a p-type light absorber, an n-type buffer, and an n-type transparent conducting oxide layers, respectively. We deposited a 1.2 μm-thick Cu_2O layer by the electrochemical deposition technique, as this produces a highly roughened surface morphology with anti-reflection properties, resulting in improved photo-generated carrier collection.[31] Conformal depositions of 5 nm-thick a-ZTO and 80 nm-thick ZnO:Al layers were followed by atomic layer deposition. The Zn-to-Sn ratio in the a-ZTO layer was adjusted to 1/0.27 to reduce interfacial recombination between Cu_2O and ZnO:Al layers.[32] As a comparison, we also fabricated a control device using the same geometry, but without the Cu_2O:N layer.

To investigate the effect of a Cu_2O:N layer in the device, current density–bias voltage (*J*–*V*) characteristics were measured. Fig. 3b shows *J*–*V* curves of two devices under dark conditions. The device with a Cu_2O:N layer exhibited a normal rectifying behaviour. However, the control device exhibited a

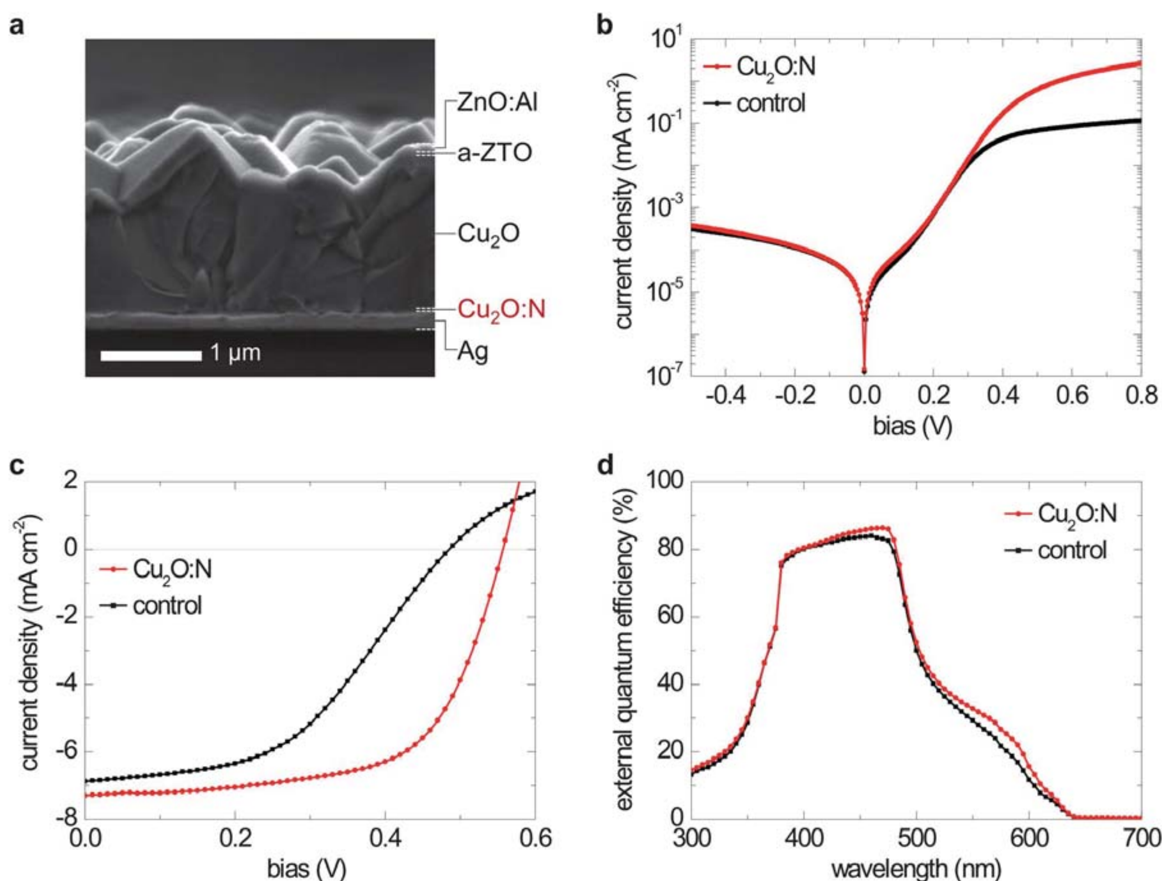

Fig. 3 (a) A cross-sectional SEM image of a Cu_2O-based thin-film solar cell with a Cu_2O:N hole-transporting layer. Dashed lines (white) indicate interfaces between layers. *J*–*V* characteristics of a Cu_2O:N-incorporated device and a control device under (b) dark and (c) 1 sun illumination (AM1.5G, 100 mW cm^{-2}) conditions. (d) External quantum efficiency of the two devices at zero-bias.

Published on 18 October 2013. Downloaded by Harvard University on 21/02/2014 20:11:26.

Published on 18 October 2013. Downloaded by Harvard University on 21/02/2014 20:11:26.

Table 1 Comparison of the photovoltaic characteristics under 1 sun (AM1.5G, 100 mW cm^{-2}) illumination

Device	V_{OC} (mV)	J_{SC} (mA cm^{-2})	FF (%)	PCE (%)
Cu_2O:N layer	557	7.3	61.0	2.56
Control	485	6.9	46.7	1.56

suppressed current density at bias voltages greater than 0.3 V, while the current density below 0.3 V was comparable with the Cu_2O:N device. Such flat *J–V* characteristics under dark conditions are often observed in CdTe thin-film solar cells with a back-contact barrier (roll-over). Those devices have been explained using a two-diode model for which a p–n junction and a leaky back-contact Schottky junction are connected in series with opposite directions.[3,33] The current density of the control device is expected to be limited by a back-contact barrier originating from the low work function of the polycrystalline Ag electrode ($\Phi_{Ag} = 4.3$ eV).[34] By inserting the Cu_2O:N layer at the Ag/Cu_2O interface, a narrow back-contact barrier can be formed in the Cu_2O:N layer, allowing a high tunnelling current through the junction. The effects of a Cu_2O:N layer on the illuminated *J–V* characteristics are shown in Fig. 3c, and their parameters are summarized in Table 1. Strong enhancements in FF and open circuit voltage (V_{OC}) were observed, resulting in a PCE of 2.56% comparable with the device with Au back-electrode.[32]

A small improvement in the short circuit current density (J_{SC}) was also observed, which was further investigated by measuring external quantum efficiency (EQE), shown in Fig. 3d. The integrated values of the EQE data with the AM1.5G spectrum match well with J_{SC} of the devices. Both devices exhibited a strong drop-off in EQE above ~490 nm, due to a sharp decrease in the optical absorption coefficient of Cu_2O. Due to the limited minority carrier collection length (~0.6 μm) of the electrochemically deposited Cu_2O layer, the photo-generated carriers originating far from the junction are only partially collected, resulting in a lower J_{SC} than the record efficiency devices.[32,35,36] The device with the Cu_2O:N layer exhibited a higher EQE relative to the control device over the wavelength range of 300–600 nm. The enhancement in EQE can be explained by the electric field in the absorber layer. Since the back-contact barrier is formed within the Cu_2O:N layer, the absorber layer contains a larger electric field over a wider collection region, thereby collecting more photo-generated carriers (Fig. 4).

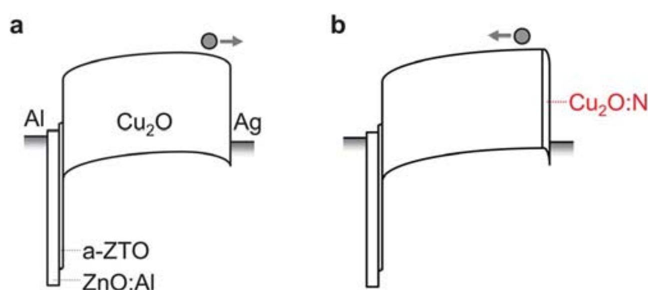

Fig. 4 Schematic diagram of band-alignments in Cu_2O-based thin-film solar cells: (a) the control device and (b) Cu_2O:N hole-transporting layer incorporated device. Circles and arrows indicate photo-generated electrons and their flow direction, respectively.

Experimental

Cu_2O:N thin-film deposition

Cu_2O:N thin-films were deposited on GE-124 quartz glass substrates by reactive magnetron sputtering using a PVD-174 sputtering system (PVD Products, Inc.). The substrate temperature was controlled using SiC heating elements. A constant power of 30 W (direct current) was applied to a 99.999% pure metallic copper target of 2 inch-dia. (K. J. Lesker Co.) to deposit 0.6 μm-thick films with a rate of 5 nm min^{-1}. The base pressure and working pressure were 1.3×10^{-5} Pa and 1.7×10^{-1} Pa, respectively.

Thin-film solar cell fabrication

A 200 nm-thick Ag bottom electrode with an underlying 5 nm-thick Ti adhesion layer was deposited on a 1 × 1 square inch SiO_2 substrate by e-beam evaporation. A 20 nm-thick Cu_2O:N film was deposited as a hole-transporting layer by sputtering. To prevent any nitrogen decomposition during the subsequent electrochemical deposition process, an additional 10 nm-thick undoped Cu_2O film was sputtered. A 1.2 μm-thick Cu_2O film as a light absorbing layer was deposited at 40 °C by the galvanostatic electrochemical deposition method.[31] A copper sulphate aqueous solution was prepared by mixing 3 M lactic acid (Sigma Aldrich) and 0.2 M cupric sulphate pentahydrate (Sigma Aldrich) in de-ionized water (Ricca Chemical). Its pH level was adjusted to 12.5 by adding 2 M sodium hydroxide (Sigma Aldrich) aqueous solution. A constant current density of 0.23 mA cm^{-2} was applied by a Keithley 2400 sourcemeter with a Pt counter electrode. 5 nm-thick amorphous ZTO and 80 nm-thick Al-doped ZnO films were deposited by atomic layer deposition using Sn(II)(1,3-bis(1,1-dimethylethyl)-4,5-dimethyl-(4*R*,5*R*)-1,3,2-diazastannolidin-2-ylidene), diethylzinc (Sigma Aldrich), and trimethylaluminum (Sigma Aldrich) as Sn, Zn, and Al precursors, respectively.[37] 50 wt% hydrogen peroxide (Sigma Aldrich) and de-ionized water were used as oxidants for a-ZTO and Al-doped ZnO deposition, respectively. The growth temperature of the oxides was 120 °C. 300 nm-thick Al electrodes with a grid spacing of 1 mm were deposited by e-beam evaporation. The cell area was defined to 3 × 5 mm^2 by photolithography and nitric acid solution wet etching.

Characterization

Nitrogen concentrations in the Cu_2O:N films were measured by SIMS (EAGLAB PCOR-SIMS^{SM}). The crystal structures of the films were characterized by XRD using a PANalytical X'Pert Pro diffractometer with Cu-Kα radiation. Surface and cross-sectional images of the films and the device were taken using a Zeiss Ultra 55 FESEM. XPS was carried out using a Kratos Analytical AXIS Nova (Korea Basic Science Institute). Samples were etched by an Ar ion beam to remove surface contaminants. The binding-energy scale was calibrated by adjusting the C 1s

This journal is © The Royal Society of Chemistry 2013

Published on 18 October 2013. Downloaded by Harvard University on 21/02/2014 20:11:26.

peak to 284.8 eV. Electrical properties of the films were characterized by temperature-dependent Hall effect measurements using the van der Pauw configuration and a magnetic field of 0.75 T. Ohmic Au contacts of 1×1 mm^2 were deposited on the corners of Cu_2O:N film samples of 1×1 cm^2. A closed-cycle He cryostat and a resistive heater were used to control the measurement temperature. Specific contact resistance was measured by preparing circular transmission line patterns with ring spacings of 4–12 μm. Film optical properties were measured using a Lambda 950 UV-VIS-NIR spectrophotometer (PerkinElmer Inc.) equipped with an integrating sphere. The J–V characteristics of the device were measured using a Keithley 2400 sourcemeter and an Agilent 4156C semiconductor characterization system. The standard 1 sun illumination was generated by a Newport Oriel 91194 solar simulator with a 1300 W Xe-lamp with an AM1.5G filter and a Newport Oriel 68951 flux controller calibrated by an NREL-certified Si reference cell equipped with a BG-39 window. The EQE of the device was measured using a QEX-7 (PV measurements, Inc.) calibrated by a NIST-certified Si photodiode.

Conclusions

In summary, we have successfully demonstrated the potential of Cu_2O:N films to serve as a hole-transporting (electron-blocking) layer in a Cu_2O-based solar cell. The nitrogen content in these films can be controlled by varying the nitrogen dose during film deposition. Nitrogen-doping can reduce electrical resistivity of the film down to 1.8×10^{-1} Ω cm by increasing the hole concentration. A 20 nm-thick Cu_2O:N film can create a tunnel junction at the positive electrode of the Cu_2O solar cell while absorbing minimal light in the subgap wavelength range. The FF and power-conversion efficiency of the device show significant enhancements relative to the control device. Cu_2O:N thin-films may also be useful in other photovoltaic material systems, improving their back-contact properties, as well as a candidate tunnel junction material for a tandem structure solar cell.

Acknowledgements

The authors thank Dr I. Kozinsky (Bosch), S. Y. Kang (MIT), M. Sher (Harvard), Dr A. Wan (EAG), and Dr J. Park (KBSI) for helpful discussions and experimental support. This work was supported by NSF CAREER award ECCS-1150878, NSF award CBET-1032955, Bosch through the MIT Energy Initiative, and the Chesonis Family Foundation. This work made use of the MTL and CMSE at MIT and the CNS at Harvard University supported by NSF awards DMR-0819762 and ECS-0335765. A Clean Energy Scholarship from NRF Singapore (S.C.S.) is acknowledged.

Notes and references

1 Z. M. Beiley and M. D. McGehee, *Energy Environ. Sci.*, 2012, **5**, 9173.
2 A. Shah, P. Torres, R. Tscharner, N. Wyrsch and H. Keppner, *Science*, 1999, **285**, 692.
3 Y. Roussillon, V. G. Karpov, D. Shvydka, J. Drayton and A. D. Compaan, *J. Appl. Phys.*, 2004, **96**, 7283.
4 D. K. Schroder and D. L. Meier, *IEEE Trans. Electron Devices*, 1984, **31**, 637.
5 D. Abou-Ras, G. Kostorz, D. Bremaud, M. Kälin, F. V. Kurdesau, A. N. Tiwari and M. Döbeli, *Thin Solid Films*, 2005, **480–481**, 433.
6 D. L. Bätzner, A. Romeo, H. Zogg, R. Wendt and A. N. Tiwari, *Thin Solid Films*, 2001, **387**, 151.
7 I. Hancox, K. V. Chauhan, P. Sullivan, R. A. Hatton, A. Moshar, C. P. A. Mulcahy and T. S. Jones, *Energy Environ. Sci.*, 2010, **3**, 107.
8 C.-P. Chen, Y.-D. Chen and S.-C. Chuang, *Adv. Mater.*, 2011, **23**, 3859.
9 V. Shrotriya, G. Li, Y. Yao, C.-W. Chu and Y. Yang, *Appl. Phys. Lett.*, 2006, **88**, 073508.
10 J. Meyer, S. Hamwi, M. Kröger, W. Kowalsky, T. Riedl and A. Kahn, *Adv. Mater.*, 2012, **24**, 5408.
11 Y. Tsur and I. Riess, *Phys. Rev. B: Condens. Matter Mater. Phys.*, 1999, **60**, 8138.
12 Y. Tsur and I. Riess, *Solid State Ionics*, 1999, **119**, 37.
13 J. Robertson and S. J. Clark, *Phys. Rev. B: Condens. Matter Mater. Phys.*, 2011, **83**, 075205.
14 L. C. Olsen, F. W. Addis and W. Miller, *Sol. Cells*, 1982, **7**, 247.
15 S. Ishizuka and K. Akimoto, *Appl. Phys. Lett.*, 2004, **85**, 4920.
16 N. Kikuchi and K. Tonooka, *Thin Solid Films*, 2005, **486**, 33.
17 S. Ishizuka, S. Kato, T. Maruyama and K. Akimoto, *Jpn. J. Appl. Phys.*, 2001, **40**, 2765.
18 C. Malerba, C. L. Azanza Ricardo, M. D'Incau, F. Biccari, P. Scardi and A. Mittiga, *Sol. Energy Mater. Sol. Cells*, 2012, **105**, 192.
19 M. Burgelman, P. Nollet and S. Degrave, *Thin Solid Films*, 2000, **361–362**, 527.
20 Y. S. Lee, M. T. Winkler, S. C. Siah, R. Brandt and T. Buonassisi, *Appl. Phys. Lett.*, 2011, **98**, 192115.
21 T. Maruyama and T. Morishita, *J. Appl. Phys.*, 1995, **78**, 4104.
22 J. Ghijsen, L. H. Tjeng, J. van Elp, H. Eskes, J. Westerink, G. A. Sawatzky and M. T. Czyzyk, *Phys. Rev. B: Condens. Matter Mater. Phys.*, 1988, **38**, 11322.
23 H. Wu and W. Chen, *J. Am. Chem. Soc.*, 2011, **133**, 15236.
24 W. H. Brattain, *Rev. Mod. Phys.*, 1951, **23**, 203.
25 L. C. Olsen, R. C. Bohara and M. W. Urie, *Appl. Phys. Lett.*, 1979, **34**, 47.
26 W.-Y. Yang and S.-W. Rhee, *Appl. Phys. Lett.*, 2007, **91**, 232907.
27 S. C. Siah, Y. S. Lee, Y. Segal and T. Buonassisi, *J. Appl. Phys.*, 2012, **112**, 084508.
28 A. Y. C. Yu, *Solid-State Electron.*, 1970, **13**, 239.
29 G. K. Reeves, *Solid-State Electron.*, 1980, **23**, 487.
30 Z. Zhao, X. He, J. Yi, C. Ma, Y. Cao and J. Qiu, *RSC Adv.*, 2013, **3**, 84.
31 P. E. de Jongh, D. Vanmaekelbergh and J. J. Kelly, *Chem. Mater.*, 1999, **11**, 3512.

32 Y. S. Lee, J. Heo, S. C. Siah, J. P. Mailoa, R. E. Brandt, S. B. Kim, R. G. Gordon and T. Buonassisi, *Energy Environ. Sci.*, 2013, **6**, 2112.
33 A. Niemegeers and M. Burgelman, *J. Appl. Phys.*, 1997, **81**, 2881.
34 M. Chelvayohan and C. H. B. Mee, *J. Phys. C: Solid State Phys.*, 1982, **15**, 2305.
35 K. P. Musselman, Y. Ievskaya and J. L. MacManus-Driscoll, *Appl. Phys. Lett.*, 2012, **101**, 253503.
36 T. Minami, Y. Nishi and T. Miyata, *Appl. Phys. Express*, 2013, **6**, 044101.
37 J. Heo, S. B. Kim and R. G. Gordon, *Appl. Phys. Lett.*, 2012, **101**, 113507.

Published on 18 October 2013. Downloaded by Harvard University on 21/02/2014 20:11:26.

 This journal is © The Royal Society of Chemistry 2013